THE $z = 2.51$ EXTREMELY RED SUBMILLIMETER GALAXY SMM J04431+0210

D. T. Frayer,[1] L. Armus,[1] N. Z. Scoville,[2] A. W. Blain,[2] N. A. Reddy,[2] R. J. Ivison,[3] and Ian Smail[4]

ABSTRACT

We report the redshift measurement for the submillimeter selected galaxy SMM J04431+0210 (N4) using the Near Infrared Spectrograph on the Keck II Telescope. The data show Hα, [N II] $\lambda\lambda$6583, 6548, and [O III] λ5007 lines at a redshift of $z = 2.51$. The high nuclear [N II]/Hα line ratio is consistent with a LINER or type II active galactic nucleus (AGN). The Hα emission is spatially resolved, suggesting the presence of significant star-forming activity outside the nucleus. From imaging with the Near Infrared Camera on the Keck I Telescope, we find an extremely red near-infrared color of $J-K = 3.2$ for N4. Follow-up redshifted CO(3→2) observations with the Owens Valley Millimeter Array constrain the mass of molecular gas to be less than 4×10^{10} $M_\odot$, after correcting for lensing. The CO-to-submillimeter flux limit, the spectroscopic line ratios, and the spectral energy distribution for N4 are all within the range of properties found in other high-redshift submillimeter sources and local ultraluminous infrared galaxies. After the correction for lensing, N4 is the weakest intrinsic submillimeter-selected source with a known redshift and represents the first redshift for the under 2 mJy 850 μm sources that are responsible for the bulk of the emission from the submillimeter population as a whole. We argue that N4 contains either an AGN or LINER nucleus surrounded by an extended region of active star formation.

Key words: galaxies: active — galaxies: evolution — galaxies: formation — galaxies: individual (SMM J04431+0210) — galaxies: starburst

1. INTRODUCTION

Since the discovery of the submillimeter population of galaxies (Smail, Ivison, & Blain 1997; Hughes et al. 1998; Barger et al. 1998; Eales et al. 1999), extensive follow-up observations across the entire electromagnetic spectrum ranging from X-ray to radio wavelengths have been obtained (see review by Blain et al. 2002). Despite these observational efforts, fundamental questions remain about the population as a whole; foremost among these are the redshift distribution and dominant energy source heating the dust. Detailed studies of individual submillimeter galaxies are crucial in answering these questions; however, progress has been slow since many submillimeter sources are extremely faint in their observed optical bands. Several of the original potential bright optical counterparts are now suspected to be misidentifications based on deep near-infrared observations (Smail et al. 1999; Frayer et al. 2000; Dunlop et al. 2003) and redshift estimates based on radio data (Smail et al. 2000; Webb et al. 2003).

The current data show that the submillimeter population has a mixture of active galactic nucleus (AGN) and starburst characteristics with properties that are roughly consistent with those of the local population of ultraluminous ($L > 10^{12}$ $L_\odot$) infrared galaxies (ULIRGs). The molecular CO line data for the submillimeter galaxies show the presence of sufficient molecular gas to fuel high levels of star formation activity (Frayer et al. 1998, 1999). However, the relative importance of AGNs and starburst activity in powering the high luminosities of the submillimeter population is still open to debate, as is the case with local ULIRGs (e.g., Sanders & Mirabel 1996; Genzel et al. 1998; Veilleux, Kim, & Sanders 1999). In order to understand the nature of the submillimeter population, we have been carrying out multiwavelength observations of individual systems in the SCUBA Cluster Lens Survey (Smail et al. 2002). This survey consists of 15 background submillimeter sources identified from sensitive submillimeter mapping of seven massive, lensing clusters. The advantage of this sample is that the amplification of the background sources allows for deeper source frame observations.

In this paper we report a redshift of $z = 2.5092 \pm 0.0008$ for the submillimeter galaxy SMM J04431+0210 (N4), obtained from near-infrared observations with the NIRSPEC instrument on the Keck II Telescope. The galaxy N4 at $04^h43^m07^s1$, $+02°10'25''$ (J2000.0) was previously identified as the likely submillimeter counterpart based on its extremely red $I-K$ color (Smail et al. 1999). An increasing number of submillimeter sources are now believed to be extremely red objects (EROs, $R-K > 6$) because of their high dust content (Smail et al. 1999; Gear et al. 2000; Lutz et al. 2001; Ivison et al. 2001; Wehner, Barger, & Kneib 2002). Since N4 is the brightest K-band (2.2 μm) ERO counterpart in the Cluster Lens Survey, it is an ideal candidate for testing whether redshifts can be obtained for the SCUBA population in the near-infrared. In addition, N4 has a 850 μm flux density of only 1.6 mJy, after correcting for lensing, making it one of the intrinsically weakest submillimeter sources yet identified. Studies of weak submillimeter sources such as N4 are crucial to our understanding of the population as a whole since the majority of the submillimeter background arises from sources with $S(850\mu m) < 2$ mJy (Blain et al. 1999a; Cowie, Barger, & Kneib 2002). We also report on follow-up CO observations with the OVRO Millimeter Array to search for molecular gas, as well as optical spectroscopy with the

[1] *SIRTF* Science Center, Mail Stop 220-06, California Institute of Technology, Pasadena, CA 91125.

[2] Department of Astronomy, Mail Stop 105-24, California Institute of Technology, Pasadena, CA 91125.

[3] Astronomy Technology Centre, Royal Observatory, Blackford Hill, Edinburgh EH9 3HJ, Scotland, UK.

[4] Institute for Computational Cosmology, University of Durham, South Road, Durham, DH1 3LE, England, UK.

TABLE 1
Observational Log

UT Date(s)	Telescope	Instrument	Line, Continuum	Integration Time (minutes)
1999 Oct 01	Keck I	NIRC	2.2 μm	10
2000 Dec 26....................	Keck II	NIRSPEC	Hα	130
2001 Jan–May................	OVRO	3 mm SIS Mixer	CO(3→2), 3 mm	1380
2001 Aug 29	Keck I	NIRC	2.2 μm	12
2001 Aug 29–31..............	Keck I	NIRC	1.2 μm	74
2002 Aug 08–09..............	Keck II	ESI	Lyα	110
2002 Aug 16	Keck II	NIRSPEC	[O III], Hβ	70

ESI instrument on the Keck II Telescope to search for additional rest-frame optical and ultraviolet (UV) emission lines. The observations presented in this paper are summarized in Table 1.

A cosmology of $H_0 = 70$ km s^{-1} Mpc^{-1}, $\Omega_M = 0.3$, and $\Omega_\Lambda = 0.7$ is assumed throughout this paper. We adopt the lensing amplification factor of $f = 4.4$, which was derived by Smail et al. (1999) and includes both the amplification due to the foreground cluster potential and the spiral galaxy near the position of N4.

2. OBSERVATIONS AND DATA REDUCTION

2.1. Spectroscopy

N4 was observed with the Near Infrared Spectrograph (NIRSPEC) on Keck II[5] on 2000 December 26. NIRSPEC is a spectrograph operating over 0.95 to 5.4 μm (McLean et al. 1998). Observations were obtained in low-resolution mode ($R \sim 1500$) with a 0″.76 (4 pixel) wide slit. The seeing was typically 0″.5 during the spectroscopic observations. The 42″ length slit was placed at a position angle of $-14°$ to contain both N4 and the core of the bright nearby galaxy 3″.1 from N4 (Fig. 1). We used the NSPEC7 filter to search the entire K-band and obtained 130 minutes of useful on-source integration. Hα emission was detected at $z = 2.51$ (§ 3.1).

In 2002 August we followed up the K-band detection of Hα by searching for the [O III] $\lambda\lambda5007$, 4959 doublet and Hβ line in H band using NIRSPEC. We used the same slit setup as done previously for K band. The NSPEC6 filter was used since it is optimized on the redward side of H band at the wavelengths of the redshifted emission lines.

The NIRSPEC data were combined in pairs at two different positions along the slit. This provided a zeroth-order background subtraction, as well as removing the dark and bias levels from the data. Pixel-to-pixel gain variations were removed by dividing by a normalized flat produced from halogen lamp images. The spectra were transformed to produce a linear spatial and wavelength scale using standard tasks in the IRAF LONGSLIT package.[6] Observations of a star nodded along the slit provided spatial calibration, while neon and argon arc lamp lines, as well as skylines provided wavelength calibration. A linear background was subtracted from the frames as a function of wavelength to remove time variations in the sky emission. The spectra of bright calibration stars were used to correct for variations in the detector response as a function of wavelength.

Given its proximity, residual light from the nearby galaxy is present in the extracted spectrum of N4 after standard data reduction. In order to obtain the true continuum level and spectral slope for N4, the wings of the galaxy light were subtracted from N4 as a function of wavelength. There is a natural trade-off between the signal-to-noise ratio (S/N) of the final spectrum and the wavelength resolution over which the subtraction is done. We smoothed over two resolution elements in wavelength for the galaxy subtraction, which left a slight residual narrow Paschen-α emission line from the foreground galaxy ($z = 0.18$) at 2.1 μm. The resulting continuum level of the K-band spectrum was calibrated by averaging over the emission from 2 to 2.4 μm and placed on the K-band magnitude scale derived from the NIRC imaging (§ 2.2). The absolute flux level of the H-band spectrum was calculated using the continuum levels of the bright nearby galaxy and N4 at 2.0 μm, where the H- and K-band spectra have overlapping wavelength coverage.

In 2002 August we also obtained follow-up spectroscopy observations with the Echellette Spectrograph and Imager (ESI) instrument (Sheinis et al. 2002) on Keck II to search for additional emission lines in the rest-frame ultraviolet and optical bands. The ESI data were taken in the high-resolution echelle mode, which provided wavelength coverage from 3900 to 1100 Å at a resolution of approximately 11 km s^{-1}. A slit with a width of 1″.25 was used. The ESI optical spectra were calibrated using the spectrophotometric standard Feige 110 (Massey et al. 1988).

2.2. Near-Infrared Imaging

We observed N4 using the Near Infrared Camera (NIRC) on Keck I in 1999 October in K band and 2001 August in J and K band. NIRC employs a 256×256 pixel InSb detector with a pixel scale of 0″.15 (Matthews & Soifer 1994). The standard K-band filter was used instead of the bluer K_s filter,

[6] IRAF is distributed by the National Optical Astronomy Observatory, which is operated by the Association of Universities for Research in Astronomy, Inc., under cooperative agreement with the National Science Foundation.
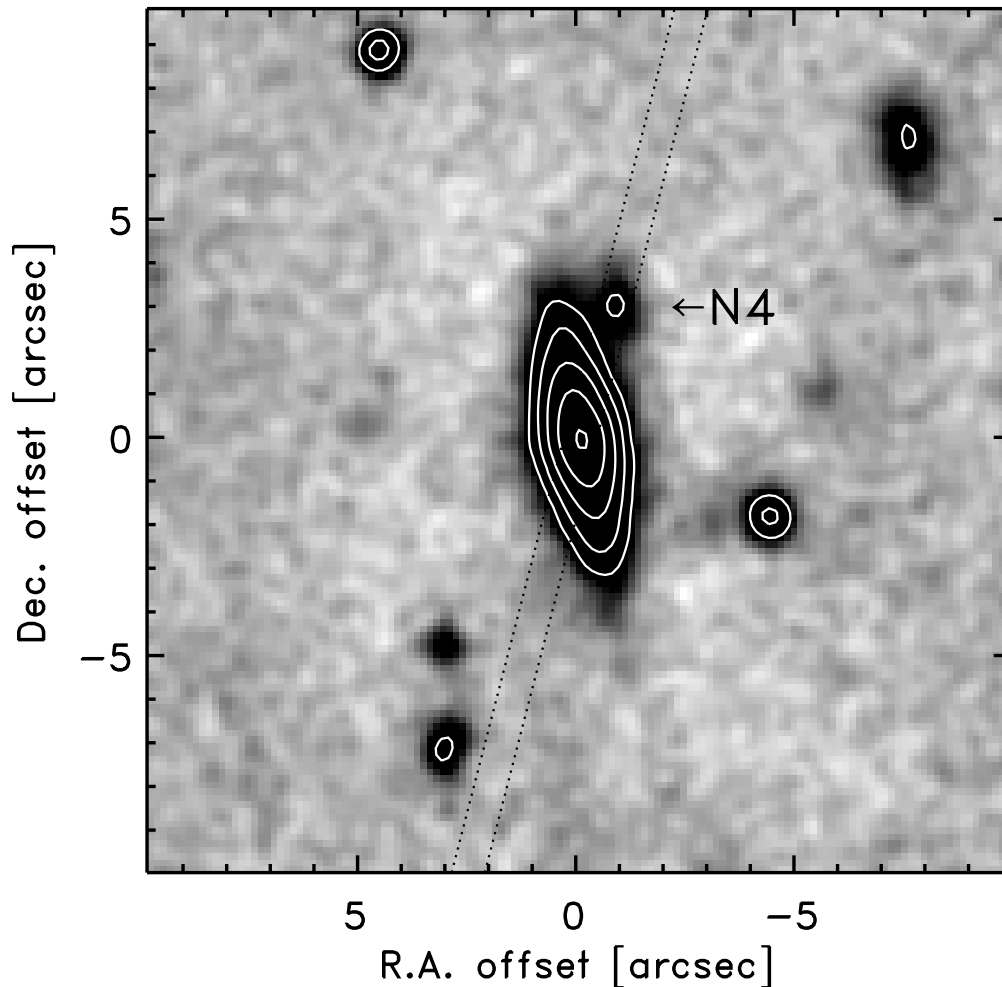
FIG. 1.—Keck K-band (2.2 μm) image of N4. The slit location for the NIRSPEC spectroscopic observations is shown by the dotted lines. The gray scale is plotted on a logarithmic scale, and the contour levels are separated by a factor of 2 in flux density, starting at the 15 σ level.

since the object is extremely red. We observed using a random dithered pattern with about $10''$ between adjacent dither positions. Integrations of 60 s were taken at each position. A total of 22 and 74 minutes of on-source data were obtained in the K and J filters, respectively. The seeing disks of the stars observed throughout the exposures varied from about $0''.5$ to $0''.7$ (FWHM).

Sets of dark frames from each night were subtracted from each exposure to remove the dark current, as well as the bias level. The dark-subtracted exposures were divided by a normalized sky flat. Frames were sky-subtracted using temporally adjacent images. Individual exposures were aligned to the nearest pixel using common objects in the frames. The data were placed on the Vega-magnitude scale from observations of a set of near-infrared standard stars (Persson et al. 1998) taken at a range of air masses to correct for atmospheric extinction. Based on the dispersion in the zero points derived throughout the nights, the uncertainty of the derived magnitude scale is estimated to be better than 0.06 mag.

2.3. *Millimeter Interferometry*

Based on the redshift derived from the NIRSPEC observations, N4 was observed using the Owens Valley

Millimeter Array[7] to search for CO emission between 2001 January and April. A total of 23 hr of usable integration time on source was obtained in two configurations of six 10.4 m telescopes. The array configurations yielded a $6'' \times 5''$ synthesized beam adopting natural weighting. We used a digital correlator configured with 112×4 MHz channels centered on 98.5174 GHz to search for CO(3→2) emission at the corresponding Hα line redshift of $z = 2.510$. The spectral-line bandwidth corresponds to 1400 km s^{-1} ($\Delta z = \pm 0.005$), which is sufficiently large to observe the entire Hα line width, including the redshift uncertainty (§ 3.1). In addition to the CO line data, 3 mm continuum data were recorded with a bandwidth of 2 GHz. The nearby quasar J0433+053 was observed every 25 minutes for gain and phase calibration. Absolute flux calibration was determined from observations of the standard calibrator 3C 273, whose flux history is monitored by observations of Uranus and Neptune. The absolute flux calibration uncertainty for the data is approximately 15%. The data were reduced using

---

[7] The Owens Valley Millimeter Array is a radio telescope facility is operated by the California Institute of Technology and supported by NSF grant AST 99-81546.

the OVRO MMA software (Scoville et al. 1983) and standard tasks in AIPS.[8]

3. RESULTS

The identification of N4 as the submillimeter counterpart is fairly secure based on previous studies. As discussed by Smail et al. (1999), the nearby $z = 0.18$ spiral galaxy can be reliably ruled out based on its radio/submillimeter flux density ratio and its 450 μm limit. The random probability of finding a bright ERO similarly as red ($R-K > 6$) as N4 within the 3″ positional uncertainty of the SCUBA data is less than 0.1%, based on the observed ERO surface densities for $K < 20$ (Thompson et al. 1999; Smith et al. 2002). If we relax the submillimeter positional uncertainty and account for lensing, the likelihood of a chance coincidence with an ERO is still less than 1%, and no other candidate red objects are nearby. The identification of N4 as the submillimeter counterpart has recently been confirmed by the detection of CO emission from N4 at the Hα redshift with the IRAM PdB interferometer (Neri et al. 2003). The OVRO CO upper limit presented in this paper is consistent with the more sensitive PdB observations.

3.1. Spectroscopy

An emission-line complex is clearly detected in the K-band spectrum of N4 (Fig. 2), which is identified as Hα + [N II] at $z = 2.51$. We also detect evidence for a weak emission line at 1.756 μm, which corresponds to [O III] $\lambda5007$ at the Hα redshift (Fig. 3). Fits to the lines and continuum were made using the SPECFIT package in IRAF (Table 2). In fitting the Hα+[N II] line complex, we have allowed the widths and fluxes of the Hα and [N II] $\lambda6583$ lines to be free, while fixing the [N II] $\lambda6548$ line to have a flux of 30% that of [N II] $\lambda6583$. Both [N II] lines were constrained to have the

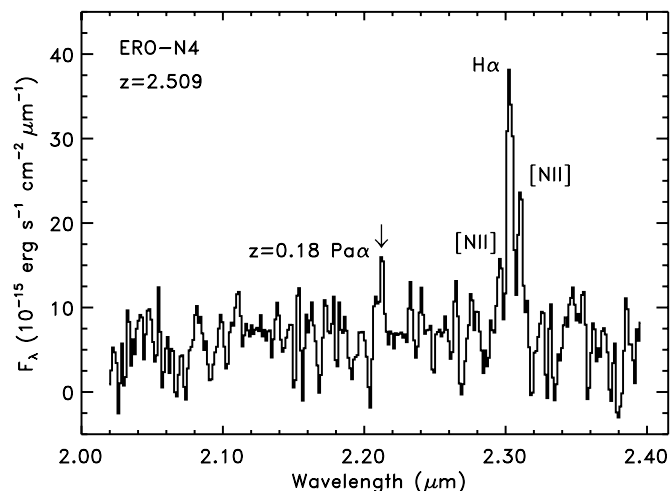FIG. 2.—Observed K-band spectrum of N4. The Hα and [N II] lines place N4 at a redshift of $z = 2.5092 \pm 0.0008$. The spectrum has been calibrated based on the K-band continuum level of N4 and has been smoothed by 26 Å. A small amount of residual Paα emission from the foreground galaxy ($z = 0.18$) remains after the subtraction of the wings of its continuum from the N4 data.
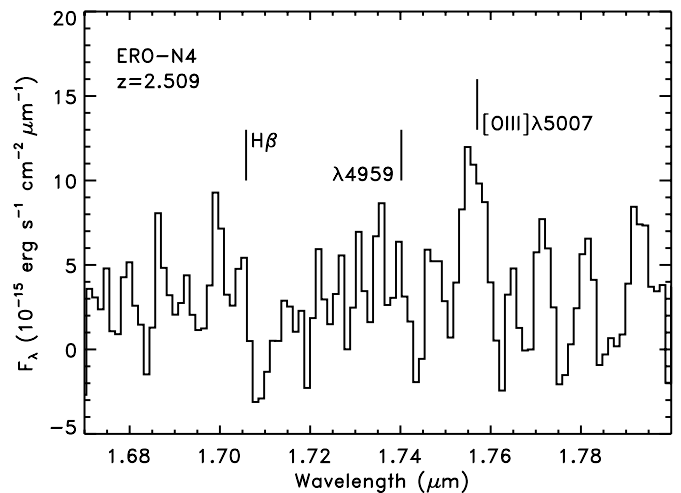

FIG. 3.—Observed H-band spectrum of N4. The [O III] $\lambda5007$ line is detected, and only upper limits can be derived at the location of the redshifted Hβ and [O III] $\lambda4959$ lines. The data have been smoothed by 25 Å.

same FWHM. The continuum was fitted with a linear function. Initially the position of the [N II] $\lambda6583$ line was fixed with respect to Hα, but this requirement was later relaxed to derive the redshift and to confirm the identification. From the fit to the total K-band spectrum, we derive a redshift of $z = 2.5092 \pm 0.0008$ based on the Hα and N II $\lambda6583$ lines. The redshift uncertainty includes the error from the fit and the systematic uncertainty associated with the derived wavelength scale. The intrinsic Hα line width is 520 ± 40 km s^{-1}, corrected for instrumental resolution, while the [N II] lines are slightly narrower, having an intrinsic FWHM of 440 ± 60 km s^{-1}. The [N II] $\lambda6583$/Hα line flux ratio is found to be 0.47 ± 0.06. No broad-line Hα component is readily visible in the data. The 1 σ upper limit on a 5000 km s^{-1} broad Hα line is about 10% of the Hα narrow-line flux.

The H-band data were fitted adopting the same techniques as used for the K-band data. The [O III] line was fitted to derive the wavelength position, line width, and line flux. In deriving the Hβ limit, we assumed the Hα redshift and linewidth. The observed limit on the [O III] $\lambda5007$/Hβ flux ratio is greater than 1.5 (3 σ).

The observed Balmer decrement of Hα/H$\beta > 6$ (3 σ) implies significant extinction. Assuming the standard intrinsic Hα/Hβ value of 2.85 (case-B Balmer recombination decrement for $T = 10^4$ K and $N_e = 10^4$ cm^{-3}; Osterbrock 1989) and the Galactic reddening function parameterized by Lequeux et al. (1979), we derive an extinction at Hα of greater than 1.6 mag and a color excess of $E(B-V) > 0.7$ mag. The high-level of extinction implied by the Hα/Hβ ratio is consistent with the nondetection of Lyα emission from the ESI observations (Table 2).

Figure 4 shows the two-dimensional image of the K-band spectrum. The Hα emission is spatially resolved, while the [N II] emission is consistent with a compact object. The size of Hα emission region is about 1″.1, after deconvolution with a Gaussian representing the seeing point-spread function. Corrected for lensing, the intrinsic diameter of the detected Hα emission regions is about 2 kpc. If the observed velocity gradient is due to rotation, a rough estimate of the dynamical mass can be made based on the Hα line width. The Hα emission is spread over 750 km s^{-1} (FWZI), and

TABLE 2
SPECTROSCOPIC PROPERTIES OF SMM J04431+0210[a]

Line	λ_{obs} (Å)	FWHM[b] (km s^{-1})	EW[c] (Å$_{rest}$)	Flux (10^{-17} ergs s^{-1} cm^{-2})
Hα	23030 ± 5	520 ± 40	66 ± 4	15.8 ± 1.0
[N II] λ6583	23102 ± 5	440 ± 60	32 ± 4	7.4 ± 0.9
[O III] λ5007..............	17560 ± 8	580 ± 160	41 ± 9	4.0 ± 0.8
Hβ	...	...	...	<2.7 (3 σ)[d]
Lα...........................	...	...	...	<2.2 (3 σ)[d]
CO(3→2)	...	...	...	<2.5 Jy km s^{-1} (3 σ)[d]

[a] Values calculated from fits to the unsmoothed data, uncorrected for lensing or extinction.
[b] Intrinsic FWHM corrected for instrumental resolution.
[c] Rest-frame EW.
[d] All limits assume an intrinsic 520 km s^{-1} FWHM line width found for the Hα line.

using a radius of 1.0 kpc, we calculate a dynamical mass of $3 \times 10^{10} \sin (i)^{-2} M_\odot$, where the inclination (i) is unknown. The estimated dynamical mass of N4 is comparable with masses found in the central regions of normal galaxies in the local universe.

Figure 5 shows spectra extracted from the different regions of N4. The [N II] λ6583/Hα line flux ratio varies measurably as a function of distance from the nucleus of N4. The off-nuclear data have a [N II] λ6583/Hα line flux ratio of 0.16 ± 0.06, consistent with star-forming regions, while the nuclear region has a much higher ratio of
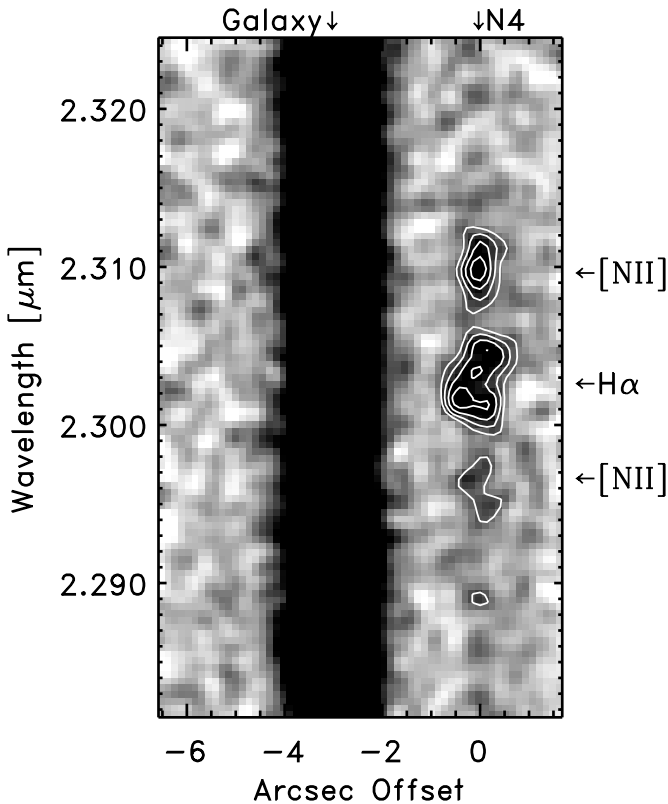

FIG. 4.—Image of the K-band spectrum of N4. The Hα emission is spatially extended, unlike the spatially unresolved [N II] λ6583 line. The extended Hα emission along with the observed line ratios suggests the association of bright star-forming regions around a central AGN and/or LINER nucleus. The contours for N4 start at 5 σ and are incremented by 2 σ.
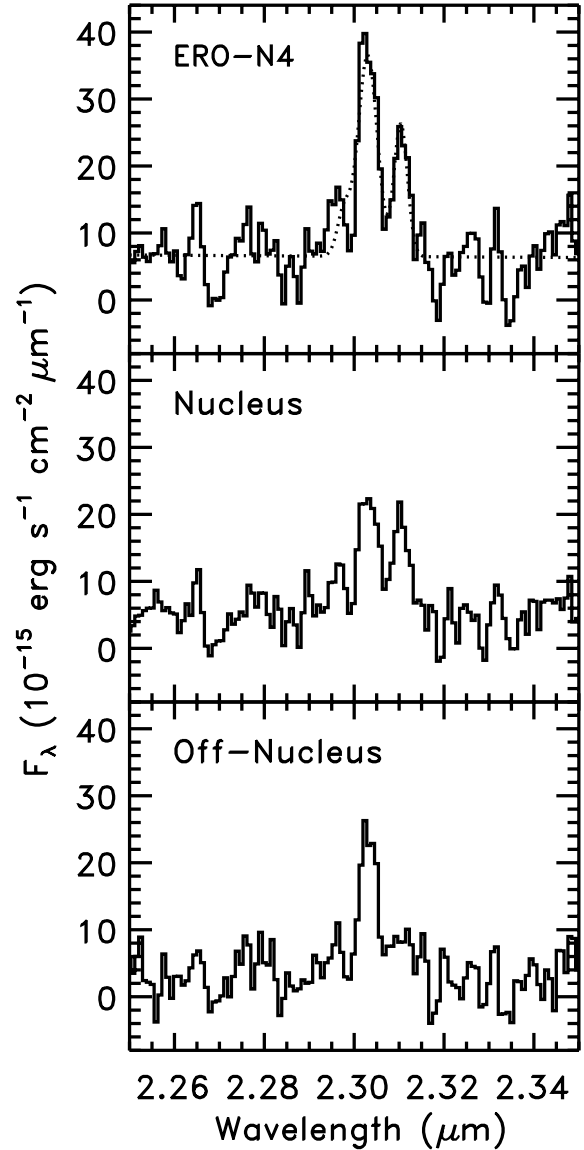

FIG. 5.—K-band spectra of N4 extracted over different spatial regions smooth over 17 Å. The top spectrum shows the total spectrum over all emission regions. The middle spectrum shows the central nucleus, while the bottom spectrum represents off-nucleus emission. The variation of the Hα/[N II] ratio suggests that N4 is a composite system with active star formation off-nucleus. The dotted line in the top spectrum shows the best-fit model to the unsmoothed data for the Hα+[N II] complex discussed in § 3.1.

0.66 ± 0.09, indicative of an AGN or a LINER (Osterbrock 1989). Therefore, the data for N4 are consistent with a narrow-line AGN surrounded by an extended region of active star formation (Baldwin, Phillips, & Terlevich 1981; Veilleux & Osterbrock 1987) or a powerful starburst with large-scale nuclear shocks driven by a nuclear superwind. (Armus, Heckman, & Miley 1989; Heckman, Armus, & Miley 1990).

3.2. *Imaging*

The sensitive *HST R*-band (F702W filter) and Keck LRIS *I*-band images of N4 have been previously discussed by Smail et al. (1999). We compare these optical images with the deep *J*- and *K*-band data presented in this paper. In all bands we subtracted the nearby galaxy using the IRAF task ELLIPSE, which enabled source masking while successfully removing the wings of the galaxy emission. The images were aligned using common sources in the frames. For optimization in *K* band, we adopted a $2''$ diameter aperture for photometry. Although the S/N from the aperture measurements in the other bands are lower than for *K* band (Table 3), the emission peak was detected in each of the four bands with a S/N greater than 5. The errors on the measurements represent the rms of multiple aperture measurements on the sky around N4, avoiding the galaxy residuals from the central disk. We measure the colors of $R-K = 6.34 \pm 0.27$ mag and $J-K = 3.15 \pm 0.29$ mag for N4. The $R-K$ measurement presented here is slightly bluer than the original $R-K > 6.7$ color quoted by Smail et al. (1999), which is attributed to the difference in the adopted aperture size and methods of galaxy subtraction.

We have resolved N4 in both the *R*- and *K*-band images (Fig. 6). After deconvolution of the $0''.6$ stellar PSF, approximated by a Gaussian, we derive a FWHM size of $1''.1 \pm 0''.2$ for the *K*-band emission, consistent with the Hα source size (§ 3.1). The *K*-band image is extended in the north-south direction, along the expected direction of lensing amplification, while the *R*-band image appears extended east-west. The *K*-band peak is marginally offset along the line of *R*-band elongation, but its derived position is coincident with the *R*-band peak within the errors. Offsets between the *K*-band and *R*-band emission regions are not unexpected given the high level of extinction within N4 and given previous results for submillimeter galaxies (Ivison et al. 2001).
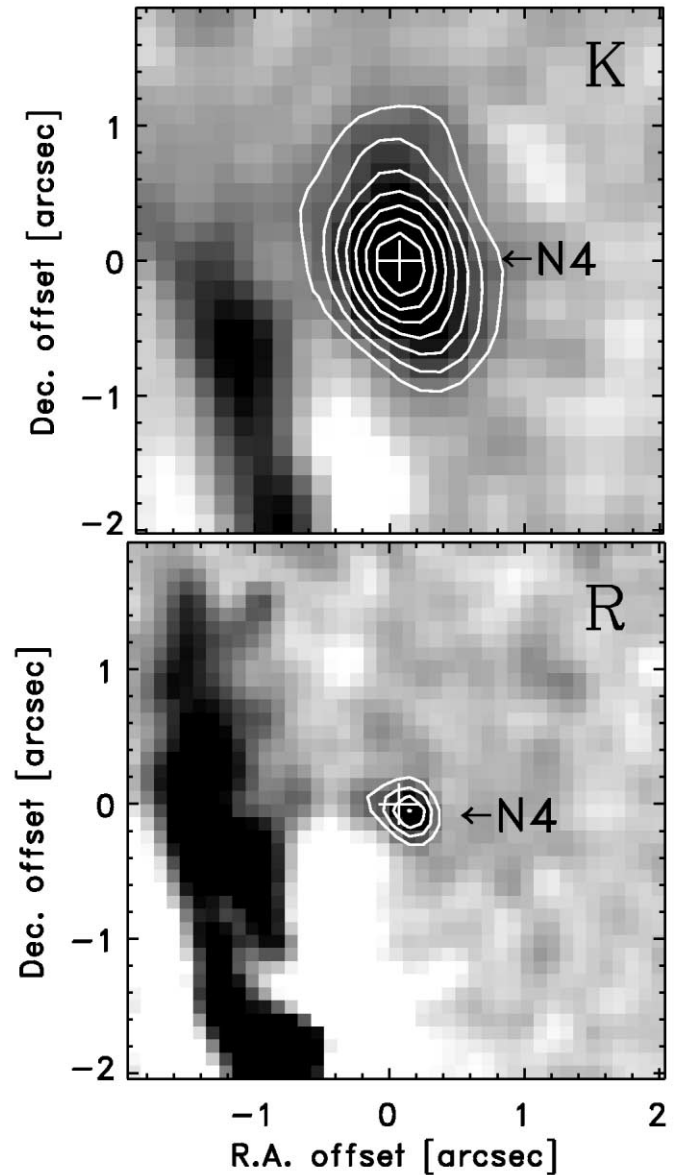

FIG. 6.—*K*- and *R*-band images of N4 after the subtraction of the wings of the bright foreground galaxy. The cross shows the position of the *K*-band peak, and its size represents the uncertainty in registering the *K*- and *R*-band data. The logarithmic gray scale is plotted from -3 to $+10$ σ, and the contour levels start at 4 σ and are incremented by 2 σ. Although the wings of the galaxy were removed, the alternating white and dark regions in the lower left of the images are due to the over- and undersubtraction of the central disk, respectively.

TABLE 3
PHOTOMETRIC PROPERTIES OF SMM J04431+0210

Observed Band[a]	Measured Value	Notes
R	25.75 ± 0.25	*HST* (F702W)
I	26.5 ± 0.6	Keck LRIS
J	22.56 ± 0.28	Keck NIRC
K	19.41 ± 0.09	Keck NIRC
850 μm	7.2 ± 1.7 mJy	Smail et al. 1999
450 μm	<60 mJy (3 σ)	Smail et al. 1999
3 mm	<1.5 mJy (3 σ)	OVRO
20 cm	<70 μJy (3 σ)	Smail et al. 1999

[a] All magnitudes are on the Vega scale, are measured with a $2''$ diameter aperture, and are uncorrected for lensing.

3.3. *Dust and Molecular Gas*

The OVRO CO observations yield a 3 σ upper limit of 4.5 mJy beam^{-1}, averaging over the Hα line width of 520 km s^{-1} with a natural-weighted beam size of $6'' \times 5''$. The limit on the integrated CO(3→2) flux density of S(CO) < 2.5 Jy km s^{-1} corresponds to a CO luminosity of $L'(CO) < 1.9 \times 10^{10}$ K km s^{-1} pc^2, correcting for lensing. The CO to H$_2$ conversion factor is still uncertain for the submillimeter population. Adopting a conversion factor of $L'(CO)/M(gas) = 2$ K km s^{-1} pc^2 ($M_\odot$ yr^{-1})$^{-1}$, which is appropriate for low-redshift ULIRGs (Solomon et al. 1997; Scoville, Yun, & Bryant 1999), the observations imply $M(gas) < 4 \times 10^{10}$ $M_\odot$ for N4. The limit on the gas mass is

comparable to the total dynamical mass estimated from the Hα line width (§ 3.1). The CO(3→2) luminosity limit is slightly lower than the previous CO detections for submillimeter selected galaxies (Frayer et al. 1998, 1999), after converting to the same cosmology, but is well within expectations given the lower 850 μm flux density for N4.

We failed to detect 3 mm continuum emission from N4, achieving a 3 σ upper limit of $S(100 \text{ GHz}) < 1.5$ mJy. The 3 mm continuum limit is consistent with the previous SCUBA measurements of N4 (Smail et al. 1999). The spectral energy distribution (SED) for N4 is consistent with those found for previous submillimeter galaxies (Ivison et al. 2000) and local ULIRGs. Based on its redshift and the limit on its 850 μm/ 1.4 GHz flux ratio, we estimate a dust temperature of $T > 40$ K from the Carilli & Yun (1999) relationship plotted as a function of temperature by Blain et al. (2002). The dust temperature is consistent with both cool and warm infrared SEDs found for ULIRGs (Soifer et al. 1989).

4. DISCUSSION

As mentioned in § 3, the rest-frame optical emission-line flux ratios of N4 imply a composite source. The relatively large nuclear [N II]/Hα and [O III]/Hβ ratios are suggestive of a nonthermal ionizing source, although we cannot rule out shock excitation from a wind. The spatially resolved Hα line emission and the lower off-nuclear [N II]/Hα ratio suggest a change to hot stars as the dominant source of ionizing photons outside the nucleus.

The observed [N II] λ6583/Hα and [O III] λ5007/Hβ line ratios for N4 are consistent with the average values found in low-redshift ULIRGs with $L_{ir} > 2 \times 10^{12} L_{\odot}$, albeit there is a large range of ratios found for local ULIRGs (Veilleux et al. 1999). The limits on the [O I] λ6300 and [S II] λλ6716, 6731 lines do not provide any additional constraints favoring one classification over another. Unfortunately, the [O I] λ6300 line for N4 is redshifted to the wavelength of the Paα from the foreground galaxy. Although there is tentative evidence for [O I] λ6300 emission even after careful galaxy subtraction, no robust measurement could be derived for this line. The Hα equivalent width (EW) and relatively narrow line width suggest that N4 does not contain a broad-line type I AGN, or that the broad-line region is heavily obscured. A higher S/N spectrum would be required to place more stringent limits on the Hα broad-line flux from N4.

The only X-ray data that currently exist for N4 are from *ROSAT*, and these data are not sensitive enough to constrain the fraction of the bolometric luminosity that may arise from an AGN. Given the unknown contribution from a possible AGN and the uncertainty in the level of extinction, the star formation rate (SFR) is fairly uncertain for N4. We can derive upper and lower bounds on the SFR based on the Hα and submillimeter emission. The off-nuclear Hα line luminosity uncorrected for extinction provides a lower limit on the SFR in N4. At the observed resolution, approximately 40% of the total Hα emission is outside the nucleus. This off-nuclear Hα emission corresponds to a line luminosity of $L(\text{H}\alpha) = 2 \times 10^8 L_{\odot}$, corrected for lensing. Adopting a standard relationship between the Hα line luminosity and the SFR (Kennicutt 1983), we find that SFR in N4 is greater than 6 $M_{\odot}$ yr^{-1}, uncorrected for extinction. Unfortunately, the Hβ limit is not sensitive enough to provide a useful estimate of the

extinction level outside the nucleus. For comparison, the total Hα line luminosity corrected for the extinction found from the limit on the Balmer decrement would imply a total SFR of greater than 70 $M_{\odot}$ yr^{-1}.

A upper limit to the SFR can be derived by assuming that all the far-infrared (FIR) radiation is due to star formation, neglecting any contribution due to a possible AGN. The FIR luminosity for N4 is derived assuming that its SED is somewhere between that of the infrared-warm ULIRG Mrk 231 and the infrared-cool ULIRG Arp 220. Placing these ULIRGs at the redshift of N4 and scaling to the delensed 850 μm flux of N4, we estimate an intrinsic FIR luminosity of $L(\text{FIR}) = 2$–$5 \times 10^{12} L_{\odot}$ for N4. This FIR luminosity corresponds to a SFR of massive stars of SFR($M > 5$ $M_{\odot}$) $\simeq 200$–500 $M_{\odot}$ yr^{-1}, using the relationship given by Condon (1992). Including the presence of lower mass stars with the IMF adopted by Kennicutt (1983), we obtain a total SFR $\simeq 800$–2000 $M_{\odot}$ yr^{-1}. Hence, from the Hα and submillimeter emission, the star formation rate of N4 is probably at least 100 $M_{\odot}$ yr^{-1} and could be as large as 2000 $M_{\odot}$ yr^{-1}.

Despite the high level of obscuration inferred for the submillimeter galaxies, the recent Lyα detections of radio-selected submillimeter sources by Chapman et al. (2003) suggest that significant rest-frame UV light can escape from the submillimeter sources. For N4 we failed to detect Lyα emission. The sensitivity of the ESI observations would have been sufficient to detect many of the Lyα sources seen by Chapman et al. (2003). However, given the fact that the Lyα/Hα ratio can span 3 orders of magnitudes for ULIRGs (<0.01–10; *HST* STIS observations by Surace et al. 2003), the observed limit of Lyα/Hα < 0.14 for N4 is not particularly constraining.

N4 has a composite spectrum consisting of a narrow-line AGN/LINER nucleus surrounded by a resolved starburst. Other well-studied submillimeter galaxies have shown a wide range of characteristics. The system SMM J02399−0126 at $z = 2.8$ shows an AGN spectrum (Ivison et al. 1998), which has been classified as broad absorption line QSO (Vernet & Cimatti 2001), while SMM J14011+0252 at $z = 2.6$ shows no evidence of an AGN and is thought to be dominated by star formation (Barger et al. 1999; Ivison et al. 2000). The most distant know submillimeter galaxy SMM J09431+4700 ($z = 3.3$) contains a narrow-line Seyfert 1 AGN (Ledlow et al. 2002), and the submillimeter galaxy N2 850.4 ($z = 2.4$) is a composite source (AGN+starburst) showing strong outflows and P Cygni profiles indicative of stellar winds (Smail et al. 2003). All of these submillimeter galaxies are significantly more luminous than N4 and can be classified as hyperluminous sources ($L \gtrsim 10^{13} L_{\odot}$). It may not be surprising that most these of the hyperluminous submillimeter sources contain AGNs given that this is seen at lower redshifts (e.g., Evans et al. 1998). The results for N4 suggest that even the lower luminosity submillimeter sources could also be partially powered by AGNs.

Although there is evidence for AGNs in many submillimeter sources, the bulk of the infrared light for the high-redshift submillimeter population is still thought to be dominated by star formation (Blain et al. 1999b, 2002). The X-ray data support this conclusion (Barger et al. 2001; Alexander et al. 2003; Almaini et al. 2003). The deepest X-ray data from Alexander et al. (2003) suggest that even though a significant faction of the bright submillimeter

sources contain an AGN, the AGNs typically have low luminosities and contribute negligibly to the total bolometric luminosity of the population.

In the local universe the apparent fraction of AGN-dominated ULIRGs increases at luminosities above $L_{ir} > 2 \times 10^{12} L_\odot$ (Veilleux et al. 1999). It is unclear if the high-redshift submillimeter population of galaxies will follow this trend. The relative importance of AGN and star formation activity in the submillimeter population will be constrained with future sensitive X-ray observations, *SIRTF* observations that will distinguish between infrared warm (AGN) versus cool (starburst) submillimeter galaxies and high-resolution millimeter and CO interferometric observations that will constrain gas masses and source sizes.

5. CONCLUSIONS

We report the redshift of $z = 2.51$ for the counterpart of the submillimeter galaxy N4. We have detected the Hα, [N II], and [O III] lines and present upper limits for Lyα, Hβ, and CO(3→2) lines. The line ratios and observed SED are consistent with the range of properties found in local ULIRGs. The data show that N4 is comprised of a nuclear region showing a LINER/type II AGN spectrum with an extended Hα component, presumably arising from an extended starburst. It is still unclear whether N4 is predominately powered by an AGN or star-forming activity. Future multiwavelength observations should provide better constraints on the source of its immense luminosity.

REFERENCES

Alexander, D. M., et al. 2003, AJ, 125, 383
Almaini, O., et al. 2003, MNRAS, 338, 303
Armus, L., Heckman, T. M., & Miley, G. K. 1989, ApJ, 347, 727
Baldwin, J. A., Phillips, M. M., & Terlevich, R. 1981, PASP, 93, 5
Barger, A. J., Cowie, L. L., Sanders, D. B., Fulton, E., Taniguchi, Y., Sato, Y., Kawara, K., & Okuda, H. 1998, Nature, 394, 248
Barger, A. J., Cowie, L. L., Smail, I., Ivison, R. J., Blain, A. W., & Kneib, J.-P. 1999, AJ, 117, 2656
Barger, A. J., Cowie, L. L., Steffen, A. T., Hornschemeier, A. E., Brandt, W. N., & Garmire, G. P. 2001, ApJ, 560, L23
Blain, A. W., Kneib, J.-P., Ivison, R. J., & Smail, I. 1999a, ApJ, 512, L87
Blain, A. W., Smail, I., Ivison, R. J., & Kneib, J.-P. 1999b, MNRAS, 302, 632
Blain, A. W., Smail, I., Ivison, R. J., Kneib, J.-P., & Frayer, D. T. 2002, Phys. Rep., 369, 111
Carilli, C. L., & Yun, M. S. 1999, ApJ, 513, L13
Chapman, S. C., Blain, A. W., Ivison, R. J., & Smail, I. R. 2003, Nature, 422, 695
Condon, J. J. 1992, ARA&A, 30, 575
Cowie, L. L., Barger, A. J., & Kneib, J.-P. 2002, AJ, 123, 2197
Dunlop, J. S., et al. 2003, MNRAS, submitted (astro-ph/0205480)
Eales, S., Lilly, S., Gear, W., Dunne, L., Bond, J. R., Hammer, F., Le Fèvre, O., & Crampton, D. 1999, ApJ, 515, 518
Evans, A. S., Sanders, D. B., Cutri, R. M., Radford, S. J. E., Surace, J. A., Solomon, P. M., Downes, D., & Kramer, C. 1998, ApJ, 506, 205
Frayer, D. T., et al. 1999, ApJ, 514, L13
Frayer, D. T., Ivison, R. J., Scoville, N. Z., Yun, M., Evans, A. S., Smail, I., Blain, A. W., &, Kneib, J.-P. 1998, ApJ, 506, L7
Frayer, D. T., Smail, I., Ivison, R., J., & Scoville, N. Z. 2000, AJ, 120, 1668
Gear, W. K., Lilly, S. J., Stevens, J. A., Clements, D. L., Webb, T. M., Eales, S. A., & Dunne, L. 2000, MNRAS, 316, L51
Genzel, R., et al. 1998, ApJ, 498, 579
Heckman, T. M., Armus, L., & Miley, G. K. 1990, ApJS, 74, 833
Hughes, D., et al. 1998, Nature, 394, 241
Ivison, R. J., Smail, I., Barger, A. J., Kneib, J.-P., Blain, A. W., Owen, F. N., Kerr, T. H., & Cowie, L. L. 2000, MNRAS, 315, 209
Ivison, R. J., Smail, I., Frayer, D. T., Kneib, J.-P., & Blain, A. W. 2001, ApJ, 561, L45
Ivison, R. J., Smail, I., Le Borgne, J.-F., Blain, A. W., Kneib, J.-P., Bézecourt, J., Kerr, T. H., & Davies, J. K. 1998, MNRAS, 298, 583
Kennicutt, R., C., Jr. 1983, ApJ, 272, 54
Ledlow, M. J., Smail, I., Owen, F. N., Keel, W. C., Ivison, R. J., & Morrison, G. E. 2002, ApJ, 577, L79

Lequeux, J., Peimbert, M., Rayo, J. F., Serrano, A., & Torres-Peimbert, S. 1979, A&A, 80, 155
Lutz, D., et al. 2001, A&A, 378, 70
Massey, P., Strobel, K., Barnes, J. V., Anderson, E., & Gronwall, C. 1988, ApJ, 328, 315
Matthews, K., & Soifer, B. T. 1994, Infrared Astronomy with Arrays: The Next Generation, ed. I. McLean (Dordrecht: Kluwer), 239
McLean, I. S., et al. 1998, Proc. SPIE, 3354, 566
Neri, R., et al. 2003, in preparation
Osterbrock, D., E. 1989, Astrophysics of Gaseous Nebulae and Active Galactic Nuclei, (Mill Valley, CA: University Sci.)
Persson, S. E., Murphy, D. C., Krzeminski, W., Roth, M., & Rieke, M. J. 1998, AJ, 116, 2475
Sanders, D. B., & Mirabel, I. F. 1996, ARA&A, 34, 749
Scoville, N. Z., Carlstrom, J. E., Chandler, C. J., Phillips, J. A., Scott, S. L., Tilanus, R. P. J., & Wang, Z. 1993, PASP, 105, 1482
Scoville, N. Z., Yun, M. S., & Bryant, P. M. 1997, ApJ, 484, 702
Sheinis, A. I., Bolte, M., Epps, H. W., Kibrick, R. I., Miller, J. S., Radovan, M. V., Bigelow, B. C., & Sutin, B. M. 2002, PASP, 114, 851
Smail, I., Chapman, S. C., Ivison, R. J., Blain, A. W., Takata, T., Heckman, T. M., Dunlop, J. S., & Sekiguchi, K. 2003, MNRAS, submitted (astro-ph/0303128)
Smail, I., Ivison, R. J., & Blain, A. W. 1997, ApJ, 490, L5
Smail, I., Ivison, R. J., Blain, A. W., & Kneib, J.-P. 2002, MNRAS, 331, 495
Smail, I., Ivison, R. J., Kneib, J.-P., Cowie, L. L., Blain, A. W., Barger, A. J., Owen, F. N., & Morrison, G. 1999, MNRAS, 308, 1061
Smail, I., Ivison, R. J., Owen, F. N., Blain, A. W., & Kneib, J.-P. 2000, ApJ, 528, 612
Smith, G. P., et al. 2002, MNRAS, 330, 1
Soifer, B. T., Boehmer, L., Neugebauer, G., & Sanders, D. B. 1989, AJ, 98, 766
Solomon, P. M., Downes, D., Radford, S. J. E., & Barrett, J. W. 1997, ApJ, 478, 144
Surace, J. A., et al. 2003, in preparation
Thompson, D., et al. 1999, ApJ, 523, 100
Veilleux, S., Kim, D.-C., & Sanders, D. B. 1999, ApJ, 522, 113
Veilleux, S., & Osterbrock, D. E. 1987, ApJS, 63, 295
Vernet, J., & Cimatti, A. 2001, A&A, 380, 409
Webb, T. M., et al. 2003, ApJ, 587, 41
Wehner, E. H., Barger, A. J., & Kneib, J.-P. 2002, ApJ, 577, L83